



Published in final edited form as:

*J Immunol.* 2012 June 15; 188(12): 6145–6155. doi:10.4049/jimmunol.1103660.

## Development of mature and functional human myeloid subsets in HSC engrafted NOD/SCID/IL2ryKO mice

Satoshi Tanaka<sup>\*,†,‡,§</sup>, Yoriko Saito<sup>‡</sup>, Jun Kunisawa<sup>\*,†</sup>, Yosuke Kurashima<sup>†</sup>, Taichi Wake<sup>†</sup>, Nahoko Suzuki<sup>‡</sup>, Leonard D. Shultz<sup>¶</sup>, Hiroshi Kiyono<sup>\*,†,#</sup>, and Fumihiko Ishikawa<sup>‡</sup>

<sup>\*</sup>Department of Medical Genome Science, Graduate School of Frontier Science, The University of Tokyo, Chiba, Japan

<sup>†</sup>Division of Mucosal Immunology, The Institute of Medical Science, The University of Tokyo, Tokyo, Japan

<sup>‡</sup>Research Unit for Human Disease Models, RIKEN Research Center for Allergy and Immunology, Yokohama, Japan

<sup>§</sup>Nippon Becton Dickinson Company, Tokyo, Japan

<sup>¶</sup>The Jackson Laboratory, Bar Harbor, Maine

<sup>#</sup>Core Research for Evolutional Science and Technology (CREST), Japan Science and Technology Agency, Tokyo 102-0075, Japan.

### Abstract

While physiological development of human lymphoid subsets has become well documented in humanized mice, *in vivo* development of human myeloid subsets in a xenotransplantation setting has remained unevaluated. Therefore, we investigated *in vivo* differentiation and function of human myeloid subsets in NOD/SCID/IL2ry<sup>null</sup> (NSG) mouse recipients transplanted with purified lineage<sup>-</sup>CD34<sup>+</sup>CD38<sup>-</sup> cord blood hematopoietic stem cells. At four to six months post-transplantation, we identified the development of human neutrophils, basophils, mast cells, monocytes, as well as conventional and plasmacytoid dendritic cells in the recipient hematopoietic organs. The tissue distribution and morphology of these human myeloid cells were similar to those identified in humans. Following cytokine stimulation *in vitro*, phosphorylation of STAT molecules was observed in neutrophils and monocytes. *In vivo* administration of human G-CSF resulted in the recruitment of human myeloid cells into the recipient circulation. Flow cytometry and confocal imaging demonstrated that human bone marrow monocytes and alveolar macrophages in the recipients displayed intact phagocytic function. Human BM-derived monocytes/macrophages were further confirmed to exhibit phagocytosis and killing of *Salmonella* Typhimurium upon the IFN- $\gamma$  stimulation. These findings demonstrate the development of mature and functionally intact human myeloid subsets *in vivo* in the NSG recipients. *In vivo* human myelopoiesis established in the NSG humanized mouse system may facilitate the investigation of human myeloid cell biology including *in vivo* analyses of infectious diseases and therapeutic interventions.

### Keywords

Human; Stem Cells; Cell Differentiation

---

Address correspondence and reprint requests to Fumihiko Ishikawa, Research Unit for Human Disease Models, RIKEN Research Center for Allergy and Immunology, 1-7-22 Suehiro-cho Tsurumi-ku, Yokohama, Japan 230-0045. f\_ishika@rcai.riken.jp (Phone: +81-45-503-9448; Fax: +81-45-503-9284).

**Disclosures** The authors have no financial conflicts of interest.

## Introduction

The use of genetically-modified mice have led to significant advances in biomedical research by providing insights into the role of individual genes both in normal physiology and in disease pathogenesis. However, translation of these findings into effective therapies for human diseases has been limited by the gap that exists between murine and human biology. The availability of human samples (e.g., cells and tissues), while supporting successful translation from bench research to clinical medicine, is limited by both logistic and ethical concerns.

Therefore, mice repopulated with human hematopoietic cells through xenogeneic transplantation were developed in order to directly investigate human immunohematopoietic system *in vivo*. Based on pioneering work using the Hu-PBL-SCID (1) and SCID-hu (2) systems, investigators have aimed to improve xenotransplantation models using immunodeficient strains of mice as recipients of human HSC in order to achieve long-term engraftment of multiple human hematopoietic and immune subsets (3). NOD/SCID mice, established by backcrossing the *scid* mutation onto the NOD strain background are characterized by partially-impaired innate immunity and deficient complement-dependent cytotoxicity, were the gold-standard for stable human hematopoietic stem/progenitor cell engraftment (3, 4). The ability of NOD-*scid* mice to support human HSC engraftment is associated with a human-like polymorphism in the IgV domain of the signal regulatory protein- $\alpha$  (*Sirpa*) allele in the NOD strain background resulting in the expression of SIRP- $\alpha$  with enhanced binding of human CD47 (5). The interaction between SIRP- $\alpha$  and CD47 has previously been implicated in the negative regulation of phagocytosis by macrophages through a “do not -eat-me signal” (6).

The introduction of IL2r common gamma chain mutations onto the NOD/SCID and NOD/Rag2KO backgrounds led to the generation of the NOD/SCID/ $\gamma_c^{\text{null}}$  (NOG) (7, 8) strain with a truncated IL-2R $\gamma$ , the NOD/SCID/IL2r $\gamma^{\text{null}}$  (NSG) (9, 10) strain with a complete IL-2R $\gamma$ -null mutation and BALB/c-Rag2KO/ $\gamma_c^{\text{null}}$  mice (11), resulting in more profound defects in innate immunity. *In vivo* human hematopoietic repopulation through transplantation of human CD34<sup>+</sup> or CD34<sup>+</sup>CD38<sup>-</sup> hematopoietic stem cells (HSC) in these severely immuno-compromised recipients accelerated human stem cell and immunology research by allowing higher levels of human HSC engraftment, differentiation of human T cells in the murine thymus and secondary lymphoid organs, enhanced maturation of human B cells, and human immune function *in vivo* (7-12).

Despite these advances, one of the remaining issues to be clarified in humanized mouse research has been the development of human myeloid lineage cells in the host mouse tissues. To date, we and others reported the development of human CD33<sup>+</sup> myeloid cells and myeloid subsets in NOG mice, BALB/c-Rag2KO/ $\gamma_c^{\text{null}}$  mice, and NSG mice (7, 9, 11, 13). Here, by using NSG newborns as recipients, we present *in vivo* differentiation of human myeloid subsets in the bone marrow (BM), spleen, and respiratory tract of NSG mice engrafted with purified lineage<sup>-</sup>CD34<sup>+</sup>CD38<sup>-</sup> human cord blood (CB) HSCs. Human granulocytes (neutrophils, basophils, and mast cells) and antigen presenting cells (monocytes/macrophages, conventional dendritic cells (cDCs) and plasmacytoid dendritic cells (pDCs)) developing in NSG mice exhibited characteristics of human myeloid cells including morphological features and expression of surface molecules known to be associated with the myeloid cell subsets. Moreover, human myeloid cells developing in the NSG recipients displayed functionality such as responsiveness to cytokine or TLR adjuvant and phagocytic function. The *in vivo* system supporting the development of mature human myeloid cells with intact function will facilitate the evaluation of human myeloid

development from hematopoietic stem/progenitor cells and further in vivo investigation of human myeloid cell-mediated immune responses against pathogens and malignancies as well as supporting studies of therapeutic agents.

## Materials and Methods

### Mice

NOD.Cg-*Prkdc<sup>scid</sup>IL2rg<sup>tm1Wjl</sup>/Sz* (NSG) mice were developed at The Jackson Laboratory by backcrossing a complete null mutation at the *Il2rg* locus onto the NOD.Cg-*Prkdc<sup>scid</sup>* (NOD/SCID) strain (9, 10). Mice were bred and maintained under defined flora with irradiated food at the animal facility of RIKEN and at The Jackson Laboratory according to guidelines established by the Institutional Animal Committees at each respective institution.

### Purification of human HSCs and xenogeneic transplantation

All experiments were performed with authorization from the Institutional Review Board for Human Research at RIKEN RCAI. CB samples were first separated for mononuclear cells (MNCs) by LSM lymphocyte separation medium (MP Biomedicals). CB MNCs were then enriched for human CD34<sup>+</sup> cells by using anti-human CD34 microbeads (Miltenyi Biotec) and sorted for 7AAD<sup>-</sup> lineage(hCD3/hCD4/hCD8/hCD19/hCD56)<sup>-</sup>CD34<sup>+</sup>CD38<sup>-</sup> HSCs using FACSARIA (BD Biosciences). To achieve high purity of donor HSCs, doublets were excluded by analysis of FSC-height/FSC-width and SSC-height/SSC-width. The purity of HSCs was higher than 98% after sorting. Newborn (within two days of birth) recipients received 150 cGy total body irradiation using a <sup>137</sup>Cs-source irradiator, followed by intravenous injection of 1-3 × 10<sup>4</sup> sorted HSCs via the facial vein (14). The recipient peripheral blood (PB) harvested from the retro-orbital plexus was evaluated for human hematopoietic engraftment every three to four weeks starting at six weeks post-transplantation. At four to six months post-transplantation, recipient mice were euthanized for analysis.

### Flow cytometry

Erythrocytes in the PB were lysed with Pharm Lyse (BD). Single cell suspensions were prepared from BM and spleen using standard procedures. To isolate mononuclear cells from the lung, lung tissues were carefully excised, teased apart, and dissociated using collagenase (Wako) (15). The following monoclonal antibodies were used for identifying engraftment of human hematopoietic cells in NSG recipients: anti-human CD3 V450 (clone UCHT1) and PE-Cy5 (HIT3a), -hCD4 PE-Cy5 (RPA-T4), -hCD8 PE-Cy5 (RPA-T8), -hCD11b/Mac-1 Pacific Blue (ICRF44), -hCD11c APC (B-ly6), -hCD14 Alexa700 (M5E2), APC-H7 and V450 (MφP9), -hCD15 APC (HI98) and V450 (MMA), -hCD19 PerCP-Cy5.5, PE-Cy5 and PE-Cy7 (SJ25C1), -hCD33 PE and PE-Cy7 (p67.6), -hCD34 PE-Cy7 (8G12), -hCD38 FITC and APC (HB7), -hCD45, V450 and V500 (HI30), -hCD45 AmCyan and APC-Cy7 (2D1), -hCD56 FITC (NCAM16.2) and PE-Cy5 (B159), -hCD114/G-CSFR PE (LMM741), -hCD116/GM-CSFR FITC (hGMCSFR-M1), -hCD117/c-Kit PerCP-Cy5.5 (104D2), -hCD119/IFN-γR PE (GIR-208), -hCD123/IL-3R PE and PerCP-Cy5.5 (7G3), -hCD284/TLR2 Alexa647 (11G7), -HLA-DR APC-H7 (L243), anti-mouse CD45 PerCP-Cy5.5 and APC-Cy7 (30-F11), all from BD; anti-human CD1c/BDCA-1 FITC (AD5-8E7), -hCD141/BDCA-3 FITC, PE and APC (AD5-14H12), -hCD303/BDCA-2 PE (AC144) from Miltenyi; anti-human CD115/M-CSFR PE (9-4D2-1E4), -hCD203c/E-NPP3 PE (NP4D6), -hCD284/TLR4 PE (HTA125), -hFceRI FITC (AER-37), anti-mouse CD45 Alexa700 (30-F11) from BioLegend. The labeled cells were analyzed using FACSCantoII or FACSARIA (BD).

## Morphological analysis

Cytospin specimens of FACS-purified human myeloid cells were prepared with a Shandon Cytospin 4 cytocentrifuge (Thermo Electric). To identify nuclear and cytoplasmic characteristics of each myeloid cell, cytopsin specimens were stained with 100% May-Grünwald solution (Merck) for 3 minutes, followed by 50% May-Grünwald solution in phosphate buffer (Merck) for additional 5 minutes, and then with 5% Giemsa solution (Merck) in phosphate buffer for 15 minutes. All staining procedures were performed at room temperature. Light microscopy was performed with Zeiss Axiovert 200 (Carl Zeiss).

## In vitro cytokine stimulation and phospho-specific flow cytometry

Following two-hour pre-culture at 37°C in RPMI-1640 (Sigma) containing 10% FBS, recipient BM cells were incubated for 15 minutes in medium supplemented with 100 ng/mL recombinant human interferon- $\gamma$  (rhIFN- $\gamma$ , BD), 100 ng/mL recombinant human granulocyte colony-stimulating factor (rhG-CSF, PeproTech), 100 ng/mL recombinant human granulocyte-macrophage colony-stimulating factor (rhGM-CSF, PeproTech) or 100 ng/mL recombinant human macrophage colony-stimulating factor (rhM-CSF, R&D systems), fixed for 10 minutes at 37°C with Phosflow Lyse/Fix Buffer (BD), permeabilized for 15 minutes at 4°C with 0.5  $\times$  Phosflow Perm Buffer IV (BD) and labeled using the following set of antibodies: anti-human CD3 PerCP-Cy5.5 (SK7), -hCD14 PE (M5E2), -hCD15 APC (HI98), -hCD33 PE-Cy7 (p67.6), -hCD45 V450 (HI30), anti-mouse CD45 APC-Cy7 (30-F11), and the combination of anti-human pSTAT1 Alexa488 (4a), pSTAT3 Alexa488 (4/P-STAT3), pSTAT4 Alexa488 (38/p-Stat4), pSTAT5 Alexa488 (47), and pSTAT6 Alexa488 (18/P-Stat6), all from BD. Phosphorylation of STAT molecules was analyzed using FACSCantoII (BD). Digital data were converted into heatmap using an online analysis system (Cytobank; <http://www.cytobank.org/>) (16).

## In vivo rhG-CSF treatment of humanized NSG mice

Human CB HSC-engrafted NSG recipients at four to six months post-transplantation were given rhG-CSF (PeproTech) at 300  $\mu$ g/kg subcutaneously once a day for five consecutive days. The recipients were analyzed for the frequency of hCD45<sup>+</sup>CD15<sup>+</sup>CD33<sup>low</sup> fraction (neutrophils) and hCD45<sup>+</sup>CD15<sup>-</sup>/lowCD33<sup>+</sup> fraction (monocytes and DCs) before and after rhG-CSF treatment.

## In vitro phagocytosis by human myeloid subsets

In vitro phagocytosis was examined using Fluoresbrite Yellow Green (YG) carboxylate microspheres (Polysciences). Following single cell preparation, recipient lung and BM cells were pre-cultured for two hours at 37°C in RPMI-1640 (Sigma) containing 10% FBS then incubated with fluorescent beads (particle:cell ratio = 10:1) for one hour at 37°C or 4°C and labeled with anti-mouse CD45 APC-Cy7, anti-human CD45APC and -hCD33 PE-Cy7 (all from BD) for identification of fluorescent beads<sup>+</sup> hCD45<sup>+</sup>hCD33<sup>+</sup> cells. The frequencies of observed fluorescent beads<sup>+</sup>hCD45<sup>+</sup>hCD33<sup>+</sup> cells out of total hCD45<sup>+</sup>hCD33<sup>+</sup> cells were determined. Fluorescent beads<sup>+</sup>hCD45<sup>+</sup>hCD33<sup>+</sup> human lung myeloid cells were purified using FACSAria (BD) and imaged using a laser-scanning confocal microscope (Zeiss LSM 710, Carl Zeiss). The intracellular localization of fluorescent beads was confirmed by scanning z-series sections.

## TLR analysis and In vivo LPS stimulation of humanized NSG mice

Surface expression levels of TLR2 and TLR4 were analyzed by FACSCantoII. To test the LPS-induced inflammatory response, human CB HSC-engrafted NSG recipients at four to six months post-transplantation were injected i.v. with LPS at 15 $\mu$ g/mouse. After LPS

injection, plasma was collected from 0 to 4 hours. Human cytokines IL-1 $\beta$ , IL-6, IL-8, IL-10, IL-12p70 and TNF were measured by cytometric bead array (CBA; BD).

### **IFN- $\gamma$ induced Salmonella killing activity by humanized mouse-derived monocytes/macrophages**

*Salmonella typhimurium* PhoPc strain transformed with the pKKGFP plasmid was kindly provided by J.P. Kraehenbuhl (17). *S. typhimurium* was grown shaking at 180 rpm overnight in LB supplemented with 100  $\mu$ g/mL ampicillin at 37°C. BM monocytes/macrophages were purified by FACSARIA (BD) based on the phenotypic characterization of lineage (CD3, CD7, CD16, CD19, CD56, CD123, CD235a)-negative, mouse CD45 and Ter119-negative, human CD45<sup>+</sup>CD11b<sup>+</sup>. Aliquots of (10<sup>4</sup>) human monocytes/macrophages derived from humanized mouse BM were cultured on collagen type I coated 96-well plates (BD) for 24 hours in either the presence or the absence of 1000 U/mL recombinant human IFN- $\gamma$  (BD). Then cells were infected with *S. typhimurium* at multiplicity of infection (MOI) of 20 at 37°C for 2 hours and the infection was confirmed by fluorescence microscopy (BIOREVO BZ-9000, KEYENCE). For intracellular CFU determination, cells were washed twice with PBS and lysed in 0.2% Triton-X 100 in PBS for 2 minutes and lysates were diluted and plated onto LB agar plates containing 100  $\mu$ g/mL ampicillin for colony enumeration.

### **Statistical analysis**

The numerical data are presented as means  $\pm$  s.e.m. unless otherwise noted. Where noted, two-tailed t-tests were performed and the differences with the *P* value < 0.05 were deemed statistically significant (GraphPad Prism, GraphPad).

## **Results**

### **Human myeloid lineage cells develop in NSG mice transplanted with human CB HSCs**

Recent advances in our knowledge of innate immunity reemphasize the importance of myeloid cells for sensing, capturing and processing antigens for the initiation of innate and acquired phases of immune responses. The development of human myeloid cells in HSC-engrafted NSG mice has not previously been studied in detail. To evaluate in vivo differentiation and function of human myeloid lineage cell populations, we transplanted  $1-3 \times 10^4$  purified human lineage<sup>-</sup>CD34<sup>+</sup>CD38<sup>-</sup> CB HSCs intravenously into sublethally irradiated newborn NSG mice. At four to six months post-transplantation, we confirmed high levels of human hematopoietic chimerism and multi-lineage differentiation of human immune subsets as evidenced by flow cytometry (Fig. 1A, 1B). In addition to the reconstitution of human adaptive immunity (CD3<sup>+</sup> T cells and CD19<sup>+</sup> B cells), we identified the development of human innate immune cell subsets such as CD56<sup>+</sup> NK cells and CD33<sup>+</sup> myeloid cells in the recipient mice. The frequency of human myeloid lineage cells was higher in the recipient BM (30.7  $\pm$  3.9%, n = 11) compared with the spleen (6.2  $\pm$  1.2%, n = 11, *p* < 0.0001 by paired two-tailed t-test) and PB (7.1  $\pm$  1.3%, n = 11, *p* < 0.0003) (Fig. 1B).

We then identified the subsets of human myeloid cells present in the humanized NSG recipient mice through flow cytometry. Human myeloid subsets are classified into HLA class II-negative granulocytes and class II-positive APCs. In the BM and spleen of NSG recipients at four to six months post-transplantation, we observed differentiation of both human granulocytes and APCs. Among the granulocyte lineage, human CD15<sup>+</sup>CD33<sup>low</sup>HLA-DR<sup>-</sup> neutrophils, CD117<sup>-</sup>CD123<sup>+</sup>CD203c<sup>+</sup>Fc $\epsilon$ RI<sup>+</sup> basophils, and CD117<sup>+</sup>CD203c<sup>+</sup>Fc $\epsilon$ RI<sup>low</sup>HLA-DR<sup>-</sup> mast cells were observed in the recipient BM and spleen. Analyses of APC populations found that CD14<sup>+</sup>CD33<sup>+</sup>HLA-

DR<sup>+</sup>BDCA-1<sup>-</sup>BDCA-3<sup>-</sup> monocytes, CD14<sup>-</sup>CD33<sup>+</sup>HLA-DR<sup>+</sup>BDCA-1<sup>+</sup> or BDCA-3<sup>+</sup> cDCs and CD123<sup>+</sup>BDCA-2<sup>+</sup>HLA-DR<sup>+</sup> pDCs developed in the recipients BM and spleen (Fig. 2A, 2B). The frequency of CD15<sup>+</sup>CD33<sup>low</sup>HLA-DR<sup>-</sup> neutrophils within human CD45<sup>+</sup>CD33<sup>+</sup> myeloid cells were present at the highest level in the BM (35.0 ± 5.4%, n = 10) whereas CD117<sup>+</sup>CD203c<sup>+</sup>FcεRI<sup>low</sup>HLA-DR<sup>-</sup> mast cells developed at a higher efficiency in the recipient spleen (43.3 ± 4.0% within CD45<sup>+</sup>CD33<sup>+</sup>, n = 10) (Fig. 2B). Among human APCs developing in the NSG recipients, monocytes accounted for the highest frequency in total myeloid cells both in the BM (32.6 ± 3.1%, n = 10) and spleen (25.2 ± 4.0%, n = 10). Conventional DCs are divided into two subsets according to the expression of BDCA-1 and BDCA-3. Within human CD45<sup>+</sup>CD33<sup>+</sup> myeloid cells, the frequencies of BDCA-1<sup>+</sup> DCs accounted for 6.4 ± 1.2% in BM (n = 9) and 6.7 ± 1.7% in spleen (n = 6) were significantly higher than those of BDCA-3<sup>+</sup> DCs (2.4 ± 0.3% and 2.8 ± 0.4%, respectively) (Fig. 2C). We then performed flow cytometric analysis using the same monoclonal antibodies to determine the frequencies of each myeloid subset in primary BM MNCs. Although we could not directly compare human neutrophil development, proportion of human monocytes, BDCA1<sup>+</sup> cDCs, and BDCA3<sup>+</sup> cDCs, and pDCs was similar between primary human BM and humanized mouse BM (Supplementary Fig.1). In addition to the expression analysis of cell surface molecules, we performed May-Grünwald-Giemsa staining to identify the morphology of the myeloid lineage cells developing in the NSG recipients. Human myeloid cells purified from NSG recipient BM exhibited characteristic morphological features (Fig. 2D).

### Human myeloid lineage cells developing in NSG recipients demonstrate intact functional responses to human cytokines in vitro and in vivo

We confirmed the development of various human myeloid subsets in the BM and spleen of NSG recipients, we next examined the expression of human cytokine receptors including IFN-γR, G-CSFR, GM-CSFR and M-CSFR as compared with human CB (Fig. 3A, 3B, 3C). By using human CD45<sup>+</sup>CD33<sup>+</sup> CB myeloid cells as control, we confirmed that human CD45<sup>+</sup>CD33<sup>+</sup> cells in the recipient BM expressed comparable levels of IFN-γR, G-CSFR, GM-CSFR and M-CSFR (n=5, no significant difference between humanized mouse BM and CB,  $p = 0.6444$ ,  $p = 0.0985$ ,  $p = 0.3879$  and  $p = 0.5816$ , respectively) (Fig. 3D).

To demonstrate functional responses to human cytokine stimulation at a cellular level, we examined the phosphorylation of STAT molecules using flow cytometry. Recent studies have revealed that hematopoietic cytokine receptor signaling is largely mediated by JAK kinases and STAT molecules known as the downstream transcription factors (18). BM cells from NSG recipients (n = 3) were stimulated with rhIFN-γ, rhG-CSF, rhGM-CSF or rhM-CSF in vitro for 15 minutes at 37°C. In neutrophils and monocytes, rhGM-CSF specifically induced STAT5 phosphorylation, but not irrelevant STATs (e.g., STAT4 and STAT6) (Fig. 4A,C). Additionally, rhIFN-γ and rhG-CSF induced optimal STAT phosphorylation (Fig. 4B, 4D, 4E). Indeed, rhIFN-γ stimulation resulted in intracellular STAT1, STAT3 and STAT5 phosphorylation, and rhG-CSF stimulation induced STAT3 and STAT5 phosphorylation, respectively (Fig. 4E). These results indicate that intact molecular events occur in human neutrophils and monocytes in response to recombinant human cytokines in vitro.

We next investigated in vivo cytokine response by human myeloid cells in the NSG humanized mice. Stimulation with rhG-CSF in vivo is known to induce proliferation of myeloid precursors and mobilization of myeloid subsets from BM (19). Following in vivo treatment of humanized mice by rhG-CSF for 5 days, the frequencies of hCD45<sup>+</sup>CD15<sup>+</sup>CD33<sup>low</sup> fraction (human neutrophils) and hCD45<sup>+</sup>CD15<sup>-/low</sup>CD33<sup>+</sup> fraction (human monocytes and DCs) increased in the PB (three out of three recipients) (Fig.

4F). These findings indicate that human myeloid cells developing in the humanized NSG recipients demonstrate functional cytokine response both in vivo and in vitro.

### Human inflammatory response via TLR signaling

Along with the role of cytokine receptor signaling in development and function of myeloid cells, signaling via Toll-like-receptors (TLRs) serves fundamental roles in evoking systemic inflammatory response by myeloid cells (20). We therefore analyzed the expression of TLRs in human myeloid cells developed in the engrafted NSG recipients by flow cytometry. We examined the surface expression of TLR2 and TLR4 in the human myeloid cells developed in the humanized mouse BM. TLR2 is specifically expressed in human monocytes and BDCA1<sup>+</sup> DCs, while TLR4 is expressed in the four distinct myeloid subsets, neutrophils, monocytes, BDCA1<sup>+</sup> cDCs, and BDCA3<sup>+</sup> cDCs (Fig. 5A, 5B). The expression of TLR4 was also confirmed in humanized mouse BM-derived monocytes and other myeloid subsets which has led us to investigate the in vivo response of human innate immunity against lipopolysaccharide (LPS), potent TLR4 ligand and endotoxin. To this end, we have administered 15 $\mu$ g LPS to NSG humanized mice followed by detecting human inflammatory cytokines by flow cytometry. Bead-attached antibodies for human cytokines did not detect 5000 pg/mL of mouse cytokines demonstrating that these antibodies and analyses are human-specific (Supplementary Fig.2). Of the cytokines examined, we have seen the significant elevation of plasma levels of huIL-6, huIL-8, and huTNF (Fig. 5C). Time-dependent kinetics showed that the prompt response of human innate cells to the LPS was achieved between 30 minutes and 1 hour after-injection. Consequently, humanized mice could be utilized to examine human innate immune response against infectious organisms and to predict inflammatory response provoked by the TLR ligands.

### Human myeloid cells present in NSG recipient lung exhibit functional phagocytosis

In the human immune system, myeloid cells serve an important role in immune surveillance not only in the systemic immune compartments but also in the mucosal tissues especially respiratory compartment of lung protected by both mucosal and systemic immune systems (21, 22). To examine whether functional reconstruction of human myeloid cells occurs in the lung, we evaluated the differentiation and function of human myeloid lineage cells isolated from the lungs of NSG recipients. Among human CD45<sup>+</sup> cells present in the NSG recipient lung, myeloid lineage cells constituted 20.3  $\pm$  3.8% (n = 8; a representative set of flow cytometry plots shown in Fig. 6A). The majority of human myeloid lineage cells residing in the recipient lungs were CD33<sup>+</sup>CD14<sup>+</sup>HLA-DR<sup>+</sup> monocytes/macrophages (60.9  $\pm$  5.1% within huCD45<sup>+</sup>CD33<sup>+</sup>, n = 8) (Fig. 6B).

The respiratory tract represents a major port of entry for inhaled pathogenic organisms and resident alveolar monocytes/macrophages play a major role in surveillance and immune defense. To confirm the phagocytic function of human monocytes/macrophages cells present in the lungs of NSG recipients, we performed in vitro phagocytosis assay using yellow-green (YG) fluorescent beads by flow cytometry and confocal microscopy imaging. After in vitro incubation of NSG recipient-derived human CD45<sup>+</sup> cells with 1 and 2  $\mu$ m fluorescent beads at 37°C, uptake of beads was noted in 9.0% and 7.9% of hCD45<sup>+</sup>CD33<sup>+</sup> human myeloid cells, respectively (Fig. 6C). It should be noted that uptake of fluorescent beads was observed only in hCD45<sup>+</sup>CD33<sup>+</sup> myeloid cells, but not in hCD45<sup>+</sup>CD33<sup>-</sup> lymphoid cells (Fig. 6C). This demonstrates that the fluorescent bead uptake specifically represents phagocytotic function by human lung myeloid cells, not non-specific uptake of the beads or binding or coating of the cells by the beads. The efficiency of uptake was 24.4  $\pm$  3.0% in the lung-derived hCD45<sup>+</sup>CD33<sup>+</sup> cells (n = 6, *p* = 0.001 compared with 4°C incubation by two-tailed t-test), equivalent to that in BM-derived hCD45<sup>+</sup>CD33<sup>+</sup> cells (16.6  $\pm$  2.7%, n = 4, *p* = 0.01 compared with 4°C incubation by two-tailed t-test) (Fig. 6C, 6D).

Next, phagocytosis of fluorescent beads by human myeloid cells was confirmed by direct visualization by confocal microscopy. Three-dimensional confocal imaging demonstrated intracellular localization of the fluorescent bead signal in sorted fluorescent bead (YG signal)<sup>+</sup>hCD45<sup>+</sup>CD33<sup>+</sup> human myeloid cells, confirming the internalization of microparticles by human monocytes/macrophages (Fig. 6E). Taken together, these findings demonstrate the presence of human innate immunity with intact phagocytic function in the NSG recipient lung.

### Humanized mouse BM-derived monocytes/macrophages exhibit IFN- $\gamma$ -induced phagocytosis and killing against *Salmonella typhimurium*

Myeloid subsets serve essential roles in host defense against various infectious microorganisms as a part of innate immunity. Of the various myeloid subsets discussed in the present study, monocytes and macrophages display excellent phagocytic potential and following internalization by phagolysosome formation and maturation, by the effects of oxidative and nitrosative stress, and by antimicrobial cationic peptides and enzymes (23). To evaluate future application of the humanized mouse system into infectious disease research, we examined phagocytic function of human monocytes/macrophages derived from humanized NSG BM against *S. typhimurium*. We purified mCD45<sup>-</sup>TER119<sup>-</sup>hCD45<sup>+</sup>Lin<sup>-</sup>CD11b<sup>+</sup> cells as monocytes/macrophages from the recipient BM (Fig. 7A), and cultured 10000 purified human monocytes/macrophages with *S. typhimurium* at MOI of 20 with or without pre-stimulation of human recombinant IFN- $\gamma$  at 1000 U/mL. In the five in vitro experiments, stimulation of human monocytes/macrophages with rhIFN- $\gamma$  resulted in the significantly potentiated phagocytosis and kill of *Salmonella* by the humanized mouse-derived monocytes/macrophages as evidenced by the decreased numbers of colony formation by *S. typhimurium* (at 3 hours post-infection:  $p = 0.023$ , at 12 hours post-infection:  $p = 0.091$  (n.s.) compared with control versus IFN- $\gamma$  stimulation by two-tailed t-test) (Fig. 7B). Taken together, human monocytes developed in the humanized NSG mice possess phagocytic against microbeads and bacteria and kill phagocytized bacteria presumably via signaling through cytokine receptors and TLRs.

## Discussion

In vivo reconstitution of mature and functional human myeloid cells not only facilitates in vivo examination of human innate immunity but also offers a promising platform for translational research in the areas of infectious immunity and drug development. In the present study, we have aimed to clarify that functional human myeloid cells develop in NSG humanized mice.

In the NSG recipients, we found distinct levels of reconstitution of myeloid subsets in the BM and spleen. The differential myeloid reconstitution in the humanized hematopoietic organs is comparable to that seen in the human tissues, reflecting the distinct physiological roles of each hematopoietic organ in mammals. BM acts an essential reservoir of short-lived neutrophils and monocytes that readily migrate into sites of infection and inflammation. In addition, BM neutrophils function as paracrine regulators for mobilization of HSCs via proteases, such as matrix metalloproteinase-9 (MMP9 or gelatinase B), cathepsin G and neutrophil elastase contained within intracellular granules. The spleen, a major secondary lymphoid organ, is not only the site of B cell maturation and APC interactions with T and B cells, but also is an organ supporting the development of mast cells from their progenitors (24, 25). Cross-reactivity of murine stem cell factor (SCF) with human c-kit<sup>+</sup> cells may explain the high frequency of human mast cells observed in the recipient spleen (26).

The development of human myeloid lineages is regulated by various cytokine signals (18, 27). In the present study, we directly compared the frequencies of human myeloid subsets



using humanized mouse BM and primary human BM MNCs. As to the development of human APCs, humanized mouse BM recapitulates physiological development of human monocytes and two different subtypes of cDCs. However, we could not directly compare the frequencies of human neutrophils between humanized mouse BM and primary human BM, since we have used frozen BM MNCs. According to the previous reports, the frequency of human neutrophils in the humanized mouse BM is lower than that in the primary human BM (28, 29).

Human myelopoiesis within the mouse microenvironment may occur through multiple cooperative mechanisms. First, mouse cytokines such as SCF, Flt3-ligand, G-CSF and thrombopoietin may directly stimulate human myelopoiesis by cross-reacting with their respective receptors on human hematopoietic stem and/or myeloid progenitor cells. These human myeloid cells in turn produce cytokines such as GM-CSF and IL-3, resulting in the differentiation, maturation and maintenance of human granulocytes, monocytes and DCs. At the same time, the cytokine milieu within the NSG recipient repopulated with human hematopoietic cells may not be completely sufficient, to support human hematopoiesis as evidenced by the relative paucity of human neutrophils in the recipient BM, spleen, and circulation that might suggest the requirement of human cytokine or adhesion molecules in the hematopoietic tissues of the recipients. Recent studies suggested that the induced expression of human cytokines in mouse environment may lead to enhanced differentiation and maturation of human myeloid subsets including neutrophils (30-33). In the present study, however human monocytes develop in NSG recipients despite the fact that M-CSF is exclusively produced in non-hematopoietic cells and that murine M-CSF does not cross-react with human M-CSFR. This may be attributable to the redundancy among cytokines such as M-CSF, GM-CSF and IL-3 as demonstrated in previous studies using M-CSF deficient mice (34).

As a measure of human myeloid cell function, we investigated cytokine responses in human neutrophils and monocytes developing in the NSG recipients. Consistent with the expression of cytokine receptors identified on the human myeloid cells, neutrophils and monocytes showed intact responses to human cytokines both in vivo and in vitro. Phosphorylation of STAT molecules represents a molecular event downstream of cytokine receptor activation. STAT1 is a key mediator of IFN- $\gamma$  activation of cells and an indispensable component of IFN- $\gamma$  dependent innate defense mechanisms against infections (35). The STAT3 signaling pathway is essential for G-CSF-mediated granulopoiesis (36). Specific phosphorylation of STAT5 may be essential molecular event enabling generation of granulocytes from myeloid progenitors and proliferation and survival of mature neutrophils (37). STAT4 and STAT6 are essential for mediating IL-12 and IL-4 signaling in helper T cells (38, 39). Human myeloid cells developing in humanized NSG recipients responded to human cytokines in a specific manner, as determined by the selective activation of JAK-STAT signaling pathways to corresponding cytokines.

Similar to the analysis of the expression of cytokine receptors and signaling, we showed that human myeloid subsets developing in the NSG humanized mice expressed various TLRs at the protein level. In the analysis of TLR expression in humanized mouse BM-derived cells, specific expression of TLR2 was observed in human monocytes and BDCA1<sup>+</sup> cDCs rather than neutrophils or BDCA3<sup>+</sup> cDCs. Consistent with the expression of TLR4 in human myeloid subsets, in vivo administration of LPS provoked potent human inflammatory response as demonstrated by the prompt elevation of plasma hIL-6, hIL-8, and hTNF levels. In addition to the examination of cytokine and TLR signaling in human myeloid cells, we investigated the function of human myeloid cells against bacteria to elucidate whether the humanized mouse system can be applied to the research for infectious immunity. As an example of bacterial infection, we chose *S. typhimurium*, a gram negative bacillus causing

gastrointestinal infections and invasive diseases, especially in children and immunosuppressed patients (40). IFN- $\gamma$  mediates signaling to activate monocytes and macrophages in phagocytosis (41, 42). In the analysis of colony formation by *S. typhimurium*, IFN- $\gamma$  potentiated the phagocytosis and antimicrobial activities of humanized mouse BM-derived monocytes/macrophages against this microorganism.

We observed not only systemic reconstitution of human myeloid subsets but also development of respiratory mucosal immunity in NSG humanized mice. Recent mouse studies revealed the crucial and specific roles of mucosal immunity in immune-surveillance and immunological homeostasis in the respiratory tracts (21, 22). In the recipient lung, unlike the BM or spleen, CD33<sup>+</sup>CD14<sup>+</sup>HLA-DR<sup>+</sup> macrophages were the predominant myeloid population. Frequencies of human B cells, T cells, and myeloid cells in the recipient lung were distinct from those in the recipient PB, excluding the possibility that the human myeloid cells isolated from the recipient lung are contaminating PB myeloid cells. Importantly, macrophages, the predominant human myeloid subset in the recipient lung, demonstrated intact phagocytic function. Macrophages in the NSG recipients will be compared with the recently-reported hGM-CSF and hIL-3 knock-in Rag2KO/IL2 $\gamma$ KO humanized mice showing abundant human macrophages in bronchoalveolar lavage (32). Establishment of an in vivo model of human pulmonary mucosal immunity may enable investigation of in vivo immune surveillance in the respiratory tract as well as allergic pulmonary disorders and may allow evaluation of vaccines at pre-clinical stages (43, 44).

In this study, the reconstitution of both systemic and mucosal human innate immunity was observed in the NSG humanized mice. We performed phenotypic characterization and functional evaluation of human myeloid cells developing in the recipients, including granulocytes and APCs. Humanized mice reconstituted with both lymphoid and myeloid human lineages would facilitate in vivo investigation of interactions between the lymphoid and the myeloid compartments, allowing the dissection of the coordinated human immune response at the level of the whole organism.

## Supplementary Material

Refer to Web version on PubMed Central for supplementary material.

## Acknowledgments

This work is supported by grants from Ministry of Education, Culture, Sports, Science and Technology in Japan and from Takeda Science Foundation to FI, grants from Ministry of Education, Culture, Sports, Science and Technology to HK and JK, the Program for Promotion of Basic and Applied Researches for Innovations in Bio-oriented Industry (BRAINI; to J.K.), YK is JSPS fellow, and grants from National Institute of Health, USAMRIID, and the Helmsley Foundation to LDS.

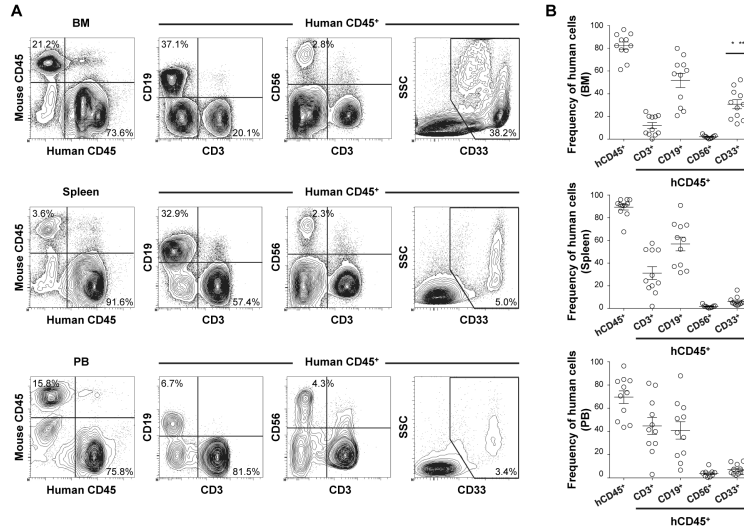
## References

1. Mosier DE, Gulizia RJ, Baird SM, Wilson DB. Transfer of a functional human immune system to mice with severe combined immunodeficiency. *Nature*. 1988; 335:256–259. [PubMed: 2970594]
2. McCune JM, Namikawa R, Kaneshima H, Shultz LD, Lieberman M, Weissman IL. The SCID-hu mouse: murine model for the analysis of human hematolymphoid differentiation and function. *Science*. 1988; 241:1632–1639. [PubMed: 2971269]
3. Greiner DL, Hesselton RA, Shultz LD. SCID mouse models of human stem cell engraftment. *Stem Cells*. 1998; 16:166–177. [PubMed: 9617892]
4. Shultz LD, Schweitzer PA, Christianson SW, Gott B, Schweitzer IB, Tennent B, McKenna S, Mobraaten L, Rajan TV, Greiner DL, et al. Multiple defects in innate and adaptive immunologic function in NOD/LtSz-scid mice. *J Immunol*. 1995; 154:180–191. [PubMed: 7995938]

5. Takenaka K, Prasolava TK, Wang JC, Mortin-Toth SM, Khalouei S, Gan OI, Dick JE, Danska JS. Polymorphism in Sirpa modulates engraftment of human hematopoietic stem cells. *Nature Immunology*. 2007; 8:1313–1323. [PubMed: 17982459]
6. Oldenborg PA, Zheleznyak A, Fang YF, Lagenaur CF, Gresham HD, Lindberg FP. Role of CD47 as a marker of self on red blood cells. *Science*. 2000; 288:2051–2054. [PubMed: 10856220]
7. Hiramatsu H, Nishikomori R, Heike T, Ito M, Kobayashi K, Katamura K, Nakahata T. Complete reconstitution of human lymphocytes from cord blood CD34+ cells using the NOD/SCID/gammacnull mice model. *Blood*. 2003; 102:873–80. [PubMed: 12689924]
8. Ito M, Hiramatsu H, Kobayashi K, Suzue K, Kawahata M, Hioki K, Ueyama Y, Koyanagi Y, Sugamura K, Tsuji K, Heike T, Nakahata T. NOD/SCID/gamma(c)(null) mouse: an excellent recipient mouse model for engraftment of human cells. *Blood*. 2002; 100:3175–3182. [PubMed: 12384415]
9. Ishikawa F, Yasukawa M, Lyons B, Yoshida S, Miyamoto T, Yoshimoto G, Watanabe T, Akashi K, Shultz LD, Harada M. Development of functional human blood and immune systems in NOD/SCID/IL2 receptor {gamma} chain(null) mice. *Blood*. 2005; 106:1565–1573. [PubMed: 15920010]
10. Shultz LD, Lyons BL, Burzenski LM, Gott B, Chen X, Chaleff S, Kotb M, Gillies SD, King M, Mangada J, Greiner DL, Handgretinger R. Human lymphoid and myeloid cell development in NOD/LtSz-scid IL2R gamma null mice engrafted with mobilized human hemopoietic stem cells. *J Immunol*. 2005; 174:6477–6489. [PubMed: 15879151]
11. Traggiai E, Chicha L, Mazzucchelli L, Bronz L, Piffaretti JC, Lanzavecchia A, Manz MG. Development of a human adaptive immune system in cord blood cell-transplanted mice. *Science*. 2004; 304:104–107. [PubMed: 15064419]
12. Legrand N, Weijer K, Spits H. Experimental models to study development and function of the human immune system in vivo. *J Immunol*. 2006; 176:2053–2058. [PubMed: 16455958]
13. McDermott SP, Eppert K, Lechman ER, Doedens M, Dick JE. Comparison of human cord blood engraftment between immunocompromised mouse strains. *Blood*. 2010; 116:193–200. [PubMed: 20404133]
14. Ishikawa F, Livingston AG, Wingard JR, Nishikawa S, Ogawa M. An assay for long-term engrafting human hematopoietic cells based on newborn NOD/SCID/beta2-microglobulin(null) mice. *Exp Hematol*. 2002; 30:488–494. [PubMed: 12031656]
15. Mega J, McGhee JR, Kiyono H. Cytokine- and Ig-producing T cells in mucosal effector tissues: analysis of IL-5- and IFN-gamma-producing T cells, T cell receptor expression, and IgA plasma cells from mouse salivary gland-associated tissues. *J Immunol*. 1992; 148:2030–2039. [PubMed: 1545116]
16. Schulz KR, Danna EA, Krutzik PO, Nolan GP. Single-cell phospho-protein analysis by flow cytometry. *Curr Protoc Immunol*. 2007 Chapter 8:Unit 8 17.
17. Niedergang F, Sirard JC, Blanc CT, Kraehenbuhl JP. Entry and survival of *Salmonella typhimurium* in dendritic cells and presentation of recombinant antigens do not require macrophage-specific virulence factors. *Proc Natl Acad Sci U S A*. 2000; 97:14650–14655. [PubMed: 11121065]
18. Baker SJ, Rane SG, Reddy EP. Hematopoietic cytokine receptor signaling. *Oncogene*. 2007; 26:6724–6737. [PubMed: 17934481]
19. Semerad CL, Liu F, Gregory AD, Stumpf K, Link DC. G-CSF is an essential regulator of neutrophil trafficking from the bone marrow to the blood. *Immunity*. 2002; 17:413–423. [PubMed: 12387736]
20. Kawai T, Akira S. The role of pattern-recognition receptors in innate immunity: update on Toll-like receptors. *Nature Immunology*. 2010; 11:373–384. [PubMed: 20404851]
21. Opitz B, van Laak V, Eitel J, Suttrop N. Innate immune recognition in infectious and noninfectious diseases of the lung. *Am J Respir Crit Care Med*. 2010; 181:1294–1309. [PubMed: 20167850]
22. Wissinger E, Goulding J, Hussell T. Immune homeostasis in the respiratory tract and its impact on heterologous infection. *Semin Immunol*. 2009; 21:147–155. [PubMed: 19223202]
23. Savina A, Amigorena S. Phagocytosis and antigen presentation in dendritic cells. *Immunol Rev*. 2007; 219:143–156. [PubMed: 17850487]

24. Arinobu Y, Iwasaki H, Gurish MF, Mizuno S, Shigematsu H, Ozawa H, Tenen DG, Austen KF, Akashi K. Developmental checkpoints of the basophil/mast cell lineages in adult murine hematopoiesis. *Proc Natl Acad Sci U S A*. 2005; 102:18105–18110. [PubMed: 16330751]
25. Hallgren J, Gurish MF. Pathways of murine mast cell development and trafficking: tracking the roots and routes of the mast cell. *Immunol Rev*. 2007; 217:8–18. [PubMed: 17498048]
26. Kambe N, Hiramatsu H, Shimonaka M, Fujino H, Nishikomori R, Heike T, Ito M, Kobayashi K, Ueyama Y, Matsuyoshi N, Miyachi Y, Nakahata T. Development of both human connective tissue-type and mucosal-type mast cells in mice from hematopoietic stem cells with identical distribution pattern to human body. *Blood*. 2004; 103:860–7. [PubMed: 14525784]
27. Manz MG. Human-hemato-lymphoid-system mice: opportunities and challenges. *Immunity*. 2007; 26:537–541. [PubMed: 17521579]
28. Brooimans RA, Kraan J, van Putten W, Cornelissen JJ, Löwenberg B, Gratama JW. Flow cytometric differential of leukocyte populations in normal bone marrow: Influence of peripheral blood contamination. *Cytometry B Clin Cytom*. 2009; 76B:18–26. [PubMed: 18942105]
29. Bjornsson S, Wahlstrom S, Norstrom E, Bernevi I, O'Neill U, Johansson E, Runstrom H, Simonsson P. Total nucleated cell differential for blood and bone marrow using a single tube in a five-color flow cytometer. *Cytometry B Clin Cytom*. 2008; 74B:91–103. [PubMed: 18061952]
30. Rathinam C, Poueymirou WT, Rojas J, Murphy AJ, Valenzuela DM, Yancopoulos GD, Rongvaux A, Eynon EE, Manz MG, Flavell RA. Efficient differentiation and function of human macrophages in humanized CSF-1 mice. *Blood*. 2011; 118:3119–28. [PubMed: 21791433]
31. Rongvaux A, Willinger T, Takizawa H, Rathinam C, Auerbach W, Murphy AJ, Valenzuela DM, Yancopoulos GD, Eynon EE, Stevens S, Manz MG, Flavell RA. Human thrombopoietin knockin mice efficiently support human hematopoiesis in vivo. *Proc Natl Acad Sci U S A*. 2011; 108:2378–83. [PubMed: 21262827]
32. Willinger T, Rongvaux A, Takizawa H, Yancopoulos GD, Valenzuela DM, Murphy AJ, Auerbach W, Eynon EE, Stevens S, Manz MG, Flavell RA. Human IL-3/GM-CSF knock-in mice support human alveolar macrophage development and human immune responses in the lung. *Proc Natl Acad Sci U S A*. 2011; 108:2390–2395. [PubMed: 21262803]
33. Takagi S, Saito Y, Hijikata A, Tanaka S, Watanabe T, Hasegawa T, Mochizuki S, Kunisawa J, Kiyono H, Koseki H, Ohara O, Saito T, Taniguchi S, Shultz LD, Ishikawa F. Membrane-bound human SCF/KL promotes in vivo human hematopoietic engraftment and myeloid differentiation. *Blood*. 2012; 119:2768–77. [PubMed: 22279057]
34. Umeda S, Takahashi K, Naito M, Shultz LD, Takagi K. Neonatal changes of osteoclasts in osteopetrosis (op/op) mice defective in production of functional macrophage colony-stimulating factor (M-CSF) protein and effects of M-CSF on osteoclast development and differentiation. *J Submicrosc Cytol Pathol*. 1996; 28:13–26. [PubMed: 8929623]
35. Hu X, Ivashkiv LB. Cross-regulation of signaling pathways by interferon-gamma: implications for immune responses and autoimmune diseases. *Immunity*. 2009; 31:539–550. [PubMed: 19833085]
36. McLemore ML, Grewal S, Liu F, Archambault A, Poursine-Laurent J, Haug J, Link DC. STAT-3 activation is required for normal G-CSF-dependent proliferation and granulocytic differentiation. *Immunity*. 2001; 14:193–204. [PubMed: 11239451]
37. Kimura A, Rieger MA, Simone JM, Chen W, Wickre MC, Zhu BM, Hoppe PS, O'Shea JJ, Schroeder T, Hennighausen L. The transcription factors STAT5A/B regulate GM-CSF-mediated granulopoiesis. *Blood*. 2009; 114:4721–4728. [PubMed: 19779039]
38. Elo LL, Jarvenpaa H, Tuomela S, Raghav S, Ahlfors H, Laurila K, Gupta B, Lund RJ, Tahvanainen J, Hawkins RD, Oresic M, Lahdesmaki H, Rasool O, Rao KV, Aittokallio T, Lahesmaa R. Genome-wide profiling of interleukin-4 and STAT6 transcription factor regulation of human Th2 cell programming. *Immunity*. 2010; 32:852–862. [PubMed: 20620947]
39. Saraiva M, Christensen JR, Veldhoen M, Murphy TL, Murphy KM, O'Garra A. Interleukin-10 production by Th1 cells requires interleukin-12-induced STAT4 transcription factor and ERK MAP kinase activation by high antigen dose. *Immunity*. 2009; 31:209–219. [PubMed: 19646904]
40. Graham SM, English M. Non-typhoidal salmonellae: a management challenge for children with community-acquired invasive disease in tropical African countries. *Lancet*. 2009; 373:267–269. [PubMed: 19150705]

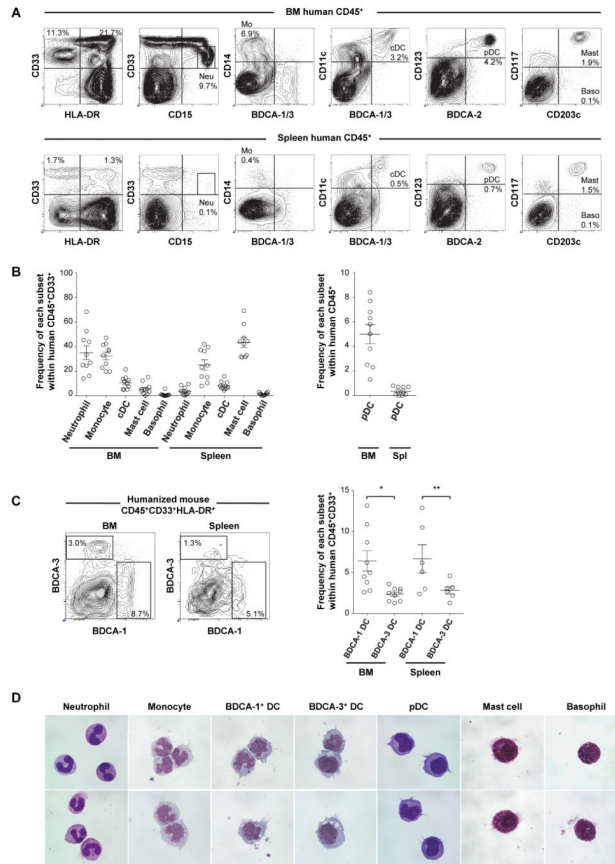
41. Liu J, Guan X, Ma X. Regulation of IL-27 p28 gene expression in macrophages through MyD88- and interferon-gamma-mediated pathways. *J Exp Med*. 2007; 204:141–152. [PubMed: 17227910]
42. MacNamara KC, Oduro K, Martin O, Jones DD, McLaughlin M, Choi K, Borjesson DL, Winslow GM. Infection-induced myelopoiesis during intracellular bacterial infection is critically dependent upon IFN- $\gamma$  signaling. *J Immunol*. 2011; 186:1032–1043. [PubMed: 21149601]
43. Jambo KC, Sepako E, Heyderman RS, Gordon SB. Potential role for mucosally active vaccines against pneumococcal pneumonia. *Trends Microbiol*. 2010; 18:81–89. [PubMed: 20031415]
44. Legrand N, Ploss A, Balling R, Becker PD, Borsotti C, Brezillon N, Debarry J, de Jong Y, Deng H, Di Santo JP, Eisenbarth S, Eynon E, Flavell RA, Guzman CA, Huntington ND, Kremsdorf D, Manns MP, Manz MG, Mention JJ, Ott M, Rathinam C, Rice CM, Rongvaux A, Stevens S, Spits H, Strick-Marchand H, Takizawa H, van Lent AU, Wang C, Weijer K, Willinger T, Ziegler P. Humanized mice for modeling human infectious disease: challenges, progress, and outlook. *Cell host & microbe*. 2009; 6:5–9. [PubMed: 19616761]



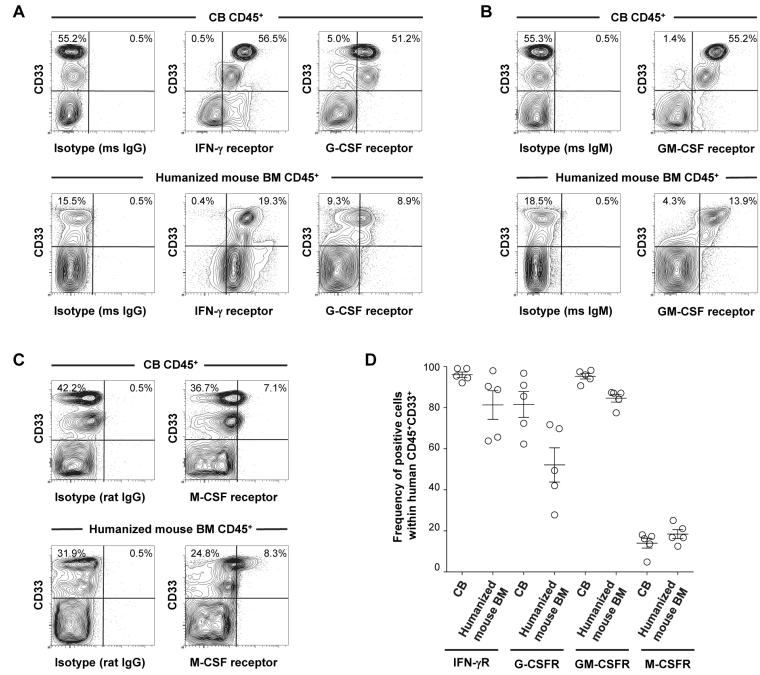
**FIGURE 1.**

Development of human acquired and innate immunity in NSG recipients following transplantation of human CB HSCs.

A, Representative sets of flow cytometry contour plots demonstrating the development of human CD45<sup>+</sup> hematopoietic cells, hCD3<sup>+</sup> T cells, hCD19<sup>+</sup> B cells, hCD56<sup>+</sup> NK cells and hCD33<sup>+</sup> myeloid cells in the BM, spleen and PB of an NSG recipient. B, Human CD45<sup>+</sup> hematopoietic chimerism and the frequencies of hCD3<sup>+</sup> T, hCD19<sup>+</sup> B, hCD33<sup>+</sup> myeloid cells (n = 11 each, frequency of myeloid cells in BM compared with spleen; \**p* < 0.0001 and PB; \*\**p* < 0.0003) and hCD56<sup>+</sup> NK (n = 9 each) cells in the BM, spleen and PB of NSG recipients at 4 to 6 months post-transplantation are summarized.



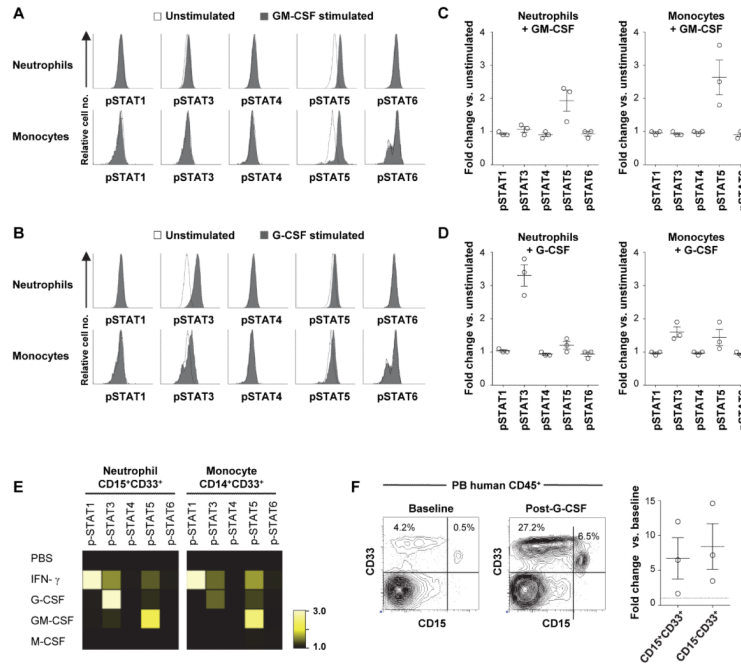
**FIGURE 2.** Development of human myeloid lineages in NSG recipients. A, Representative flow cytometry contour plots demonstrating differentiation of human HLA-DR<sup>-</sup> granulocytes and HLA-DR<sup>+</sup> APCs in the BM and spleen of an NSG recipient. B, The frequencies of human neutrophils (Neu), monocytes (Mo), cDCs, mast cells (Mast), basophils (Baso) and pDCs in the BM and spleen of NSG recipients are summarized (n = 10). C, In the humanized mouse BM and spleen, two distinct subsets of DCs, BDCA-1<sup>+</sup> DCs and BDCA-3<sup>+</sup> DCs were identified in HLA-DR<sup>+</sup>CD33<sup>+</sup>CD11c<sup>+</sup> conventional DCs. Frequencies of the two DC subsets within BM and spleen hCD45<sup>+</sup>CD33<sup>+</sup> cells are shown (BM; n=9, \**p* = 0.007, significant differences between cDCs, spleen; n=6, \*\**p* = 0.046). D, Human myeloid cells isolated by cell sorting of recipient BM demonstrate characteristic morphological features on May-Grünwald-Giemsa stain.



**FIGURE 3.**

Expression of cytokine receptors on human myeloid cells in NSG recipients. A-C, Representative flow cytometry contour plots demonstrating the expression of IFN- $\gamma$ R, G-CSFR, GM-CSFR, and M-CSFR by CB hCD45<sup>+</sup>CD33<sup>+</sup> myeloid cells (upper) and by hCD45<sup>+</sup>CD33<sup>+</sup> myeloid cells derived from humanized NSG BM (lower). Contour plots for isotype control Ig are also shown. D, Expression of each cytokine receptor within hCD45<sup>+</sup>CD33<sup>+</sup> cells is summarized (CB; n = 5, humanized NSG BM; n = 5).

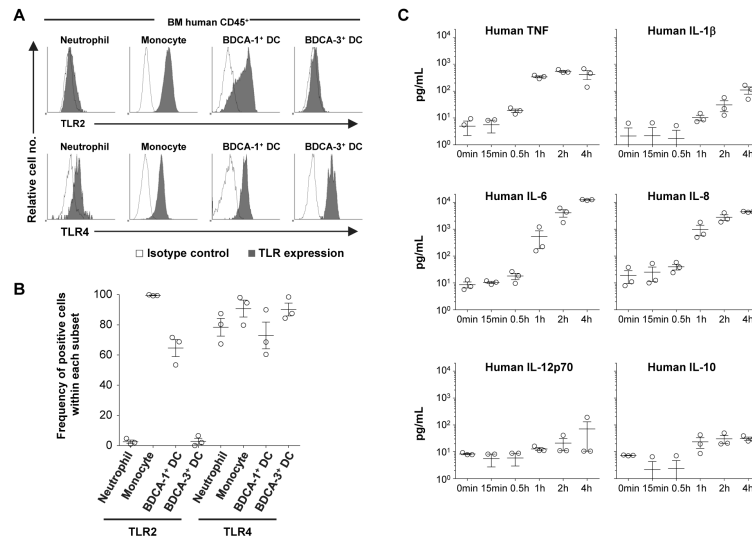




**FIGURE 4.**

Human myeloid lineage cells developing in NSG recipients demonstrate cytokine responses in vitro and in vivo.

A, B, Phosphorylation of STAT1, STAT3, STAT4, STAT5, and STAT6 in human neutrophils and monocytes derived from a NSG recipient BM following in vitro stimulation with rhGM-CSF (A) and with rhG-CSF (B) was measured by flow cytometry. C, D, Results from three independent experiments using three different recipients are summarized. E, Heatmap representation of STAT phosphorylation in human neutrophils and monocytes in an NSG recipient BM following in vitro cytokine treatment relative to PBS exposure is shown. F, Representative flow cytometry contour plots demonstrating expansion of myeloid lineage cells in the PB of an NSG recipient in response to in vivo recombinant human G-CSF administration. Frequencies of hCD45<sup>+</sup>CD15<sup>+</sup>CD33<sup>low</sup> and hCD45<sup>+</sup>CD15<sup>-/low</sup>CD33<sup>+</sup> myeloid cells were increased following in vivo rhG-CSF treatment in PB of NSG recipients for 5 days.

**FIGURE 5.**

Expression of TLRs and response to TLR adjuvant by humanized mouse-derived myeloid subsets.

TLR expression is analyzed in the granulocytes, monocytes and cDCs derived from the humanized NSG recipient BM. A, B, Expression of TLR2 and TLR4 in neutrophils, monocytes, BDCA-1<sup>+</sup> DCs, and BDCA-3<sup>+</sup> DCs was analyzed by flow cytometry. C, At different time points after the injection of 15  $\mu$ g LPS into humanized NSG recipients, human specific cytokine levels in plasma were evaluated by cytometric bead array (n = 3).

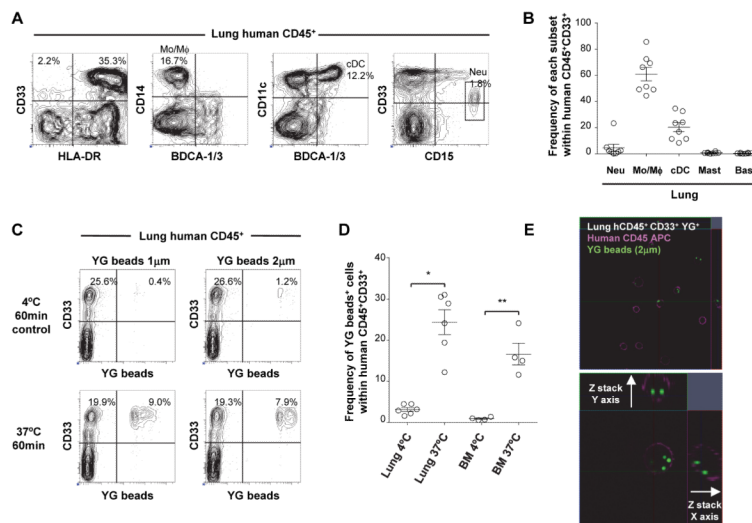


**FIGURE 6.** Human monocytes/macrophages developing in NSG recipient lung demonstrate phagocytosis of micro-particles. A, Representative contour plots demonstrating the reconstitution of human myeloid cells in the lungs of an NSG recipient. Human CD45<sup>+</sup> cells within lung cell populations were analyzed by CD33, HLA-DR, CD14, CD11c, BDCA-1/3, and CD15 to identify monocytes/macrophages ( Mo/M $\phi$ ), cDCs, and neutrophils (Neu). B, The frequencies of human neutrophils (Neu), monocytes/macrophages (Mo/M $\phi$ ), cDCs, mast cells (Mast) and basophils (Baso) within hCD45<sup>+</sup>CD33<sup>+</sup> NSG recipient lung are summarized (n = 8). C, A set of representative flow cytometry plots demonstrating the presence of hCD45<sup>+</sup>CD33<sup>+</sup>fluorescent beads<sup>+</sup> cells. D, Summary of the frequency of hCD45<sup>+</sup>CD33<sup>+</sup> fluorescent bead<sup>+</sup> cells in NSG recipient lung cell populations incubated at 37°C and at 4°C (control), respectively, with fluorescent beads (lung; n = 6, BM; n = 4, \**p* = 0.001, \*\**p* = 0.01). E, Confocal imaging of FACS-purified hCD45<sup>+</sup>CD33<sup>+</sup>fluorescent beads<sup>+</sup> cells derived from NSG recipient lung cell populations show internalization of fluorescent beads (green) within hCD45 (purple)-expressing human myeloid cells.

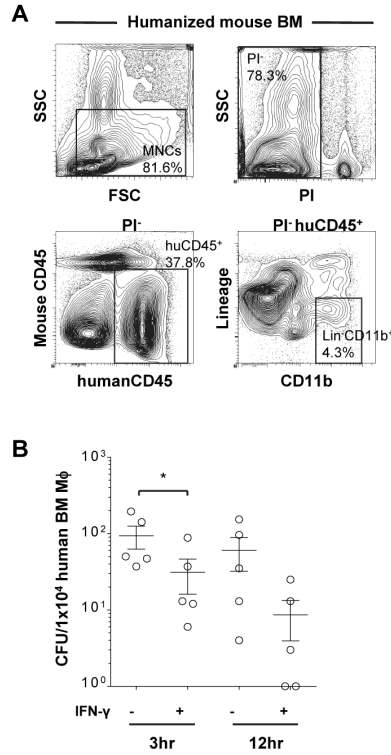


**FIGURE 7.**

Cytotoxicity against *S. typhimurium* by IFN- $\gamma$  activated human monocytes/macrophages developing in NSG recipient.

A, Within mononuclear cell gate, PI<sup>-</sup> viable, hCD45<sup>+</sup>Lin<sup>-</sup>CD11b<sup>+</sup> cells were purified from the BM of humanized NSG recipients. Purified BM monocytes/macrophages were stimulated with or without supplementation of 1000 U/mL human IFN- $\gamma$  for 24h and then infected with *S. typhimurium* at 20 MOI. B, Intracellular CFU was counted at 3 and 12 hours post-infection (n = 5, \*p = 0.023 compared with non-stimulated).